buildings

MDPI

Article

Kriging Metamodel-Based Seismic Fragility Analysis of Single-Bent Reinforced Concrete Highway Bridges

Phuong Hoa Hoang [1], Hoang Nam Phan [1,*], Duy Thao Nguyen [1] and Fabrizio Paolacci [2]

[1] Faculty of Road and Bridge Engineering, The University of Danang–University of Science and Technology, Danang 550000, Vietnam; hphoa@dut.udn.vn (P.H.H.); ndthao@dut.udn.vn (D.T.N.)
[2] Department of Engineering, University Roma Tre, 00146 Rome, Italy; fabrizio.paolacci@uniroma3.it
* Correspondence: phnam@dut.udn.vn

Abstract: Uncertainty quantification is an important issue in the seismic fragility analysis of bridge type structures. However, the influence of different sources of uncertainty on the seismic fragility of the system is commonly overlooked due to the costly re-evaluation of numerical model simulations. This paper aims to present a framework for the seismic fragility analysis of reinforced concrete highway bridges, where a data-driven metamodel is developed to approximate the structural response to structural and ground motion uncertainties. The proposed framework to generate fragility curves shows its efficiency while using a few finite element simulations and accounting for various modeling uncertainties influencing the bridge seismic fragility. In this respect, a class of single-bent bridges available in the literature is taken as a case study, whose three-dimensional finite element model is established by the OpenSees software framework. Twenty near-source records from different sources are selected and the Latin hypercube method is applied for generating the random samples of modeling and ground motion parameters. The Kriging metamodel is then driven on the structural response obtained from nonlinear time history analyses. Component fragility curves of the reinforced concrete pier column are derived for different damage states using the Kriging metamodel whose parameters are established considering different modeling parameters generated by Monte Carlo simulations. The results demonstrate the efficiency of the proposed framework in interpolating the structural response and deriving the fragility curve of the case study with any input conditions of the random variables.

Keywords: fragility analysis; kriging metamodel; reinforced concrete bridge; nonlinear time history analysis; Monte Carlo simulation

Citation: Hoang, P.H.; Phan, H.N.; Nguyen, D.T.; Paolacci, F. Kriging Metamodel-Based Seismic Fragility Analysis of Single-Bent Reinforced Concrete Highway Bridges. *Buildings* **2021**, *11*, 238. https://doi.org/10.3390/buildings11060238

Academic Editor: Xavier Romão

Received: 4 May 2021
Accepted: 29 May 2021
Published: 31 May 2021

1. Introduction

Seismic vulnerability is often represented in the form of fragility curve, which is an important decision support tool to identify the potential seismic risk in the framework of performance-based earthquake engineering (PBEE). These curves represent the conditional probability of exceeding a limit state for a given seismic intensity. In recent decades, owing to the development of the computer's hardware and numerical modeling techniques, different methods of the seismic fragility evaluation for bridge structures in highway networks, especially reinforced concrete (RC) bridges, have been extensively developed also in a parametric form in the case of bridge classes [1]. Innovative numerical models and computational techniques help to simulate and analyze complex and large structures with high accuracy; however, they are computationally expensive [2–4]. In addition, one of the challenges in the development of seismic fragility functions is to include various sources of uncertainties, e.g., ground motion and modeling parameters, into the probabilistic seismic demand model. Therefore, the fragility function may hardly be presented in closed-form, which is typically assumed as lognormal and calibrated using fitting methods or by Monte Carlo simulations.

Traditional seismic fragility assessment methods consider the record-to-record variation only to obtain component and system fragility curves [1]; this may result in an inaccurate estimation due to a deterministic assumption of input parameters such as material and geometry properties of the model. Considering different sources of uncertainty into a complex numerical model or a class of structures is commonly a hard task due to the time-consuming re-construction and re-evaluation of the numerical model. Therefore, implementing interpolation or regression techniques to accurately predict the seismic response of structural elements that only use a few numbers of dynamic analyses is an alternative in the seismic vulnerability assessment step [2–4].

With the development of the computer science industry, machine learning has evolved rapidly over recent years and widely applied to the earthquake engineering field [5]. The substantial computational time of complex finite element (FE) models can be reduced by building a surrogate model or metamodel, i.e., from the subset of machine learning techniques. This approximation modeling approach is adopted when the outcome cannot be directly measured; thus, an interpolation model of the outcome is used instead [6]. Different types of surrogate models have been previously presented, which are commonly classified into three categories, i.e., data-driven surrogates, projection-based methods, and multi-fidelity-based surrogates. The proper application of these models to different fields of engineering has also been demonstrated [7–10].

Kriging or Gaussian modeling regression is one of the data-driven surrogate models which has been widely adopted in engineering problems. The idea of this regression approach is that the value of a function at a given point can be predicted by taking a weighted average of known values of the neighborhood points, and the function of interest is treated as a realization of a Gaussian random process, whose parameters are estimated from available inputs and computer outputs [11]. The application of surrogate modeling techniques for generating seismic fragility curves has recently been used for bridges (e.g., [12,13]). Kriging metamodel has also been adopted in a few recent studies for the seismic vulnerability analysis of bridges. The possibility of the application of a Kriging metamodel to the seismic fragility evaluation of an RC bridge was presented by Zhang and Wu [14]. The performance of the Kriging metamodel in generating seismic fragility curves is verified with the conventional Latin hypercube method using a simple nonlinear spring-mass single-degree-of-freedom system. Most recently, Gidaris et al. [15] discussed the computational efficiency for fragility and resilience analyses of bridges incorporating aftershock effects. In this case, the nonlinear mainshock and aftershock bridge responses are approximately obtained using the Kriging model established from uncertain hazard and structural model parameters. In the above studies, the influence of trend and covariance models forming the metamodel has not been clarified that may have a significant effect on the predicted response. There is also the lack of detailed discussions on cross-validation methods to estimate the prediction error of a given metamodel; this is an important indicator that should be considered for assessing the model performance.

Thus, this study aims to discuss in detail a computationally efficient framework for the seismic fragility evaluation of a class of RC highway bridges based on a Kriging-based surrogate model and its flexibility in generating fragility curves for different input conditions of the modeling parameters. To reach this goal, a class of typical single-column bent RC highway bridge is selected, whose material and geometry properties are considered to be random variables. Based on a suitable design of the experiments (DOE) method, several samples are generated and corresponding three-dimensional FE models are then properly developed using the OpenSees software. The Kriging metamodel is built based on nonlinear time history responses of the FE models, in which the influence of different trend functions that form the metamodel are evaluated. Consequently, component fragility curves associated with failure modes of the column bent considering different input conditions of the modeling parameters are obtained using Monte Carlo simulations.

This paper is organized as follows. In Section 2, a description of the Kriging metamodel-based seismic fragility analysis framework of RC bridges is presented. The application of the methodology to a case study of single-bent RC highway bridges is presented in Section 3. Section 4 finishes with conclusions.

2. Kriging-Based Metamodeling

2.1. Kriging Formulation

Kriging or Gaussian process regression is a commonly used interpolation method that uses a set of observed data to predict spatially correlated data. One of the advantages of the Kriging model is its flexibility to represent a variety of complex models using a limited number of observed data. Differently from other kinds of data-driven methods (e.g., linear regression, artificial neural networks, or polynomial chaos), the Kriging model provides a function that is independent of the probabilistic model for the input data.

The Kriging model is formulated by two terms including the mean of the Gaussian process and the zero mean covariance stationary Gaussian process that is a combination of a regression model and departure [16],

$$Y(\mathbf{x}) = \boldsymbol{\beta}^T \mathbf{f}(\mathbf{x}) + Z(\mathbf{x}), \tag{1}$$

where $Y(\mathbf{x})$ is the unknown function of interest, $\mathbf{f}(\mathbf{x})$ is the known regression function vector, $\boldsymbol{\beta}$ is the unknown regression coefficient vector. The team $\boldsymbol{\beta}^T \mathbf{f}(\mathbf{x})$ in Equation (1) refers to the mean of a Kriging metamodel known as the trend. The most commonly used trends based on a polynomial basis are listed such as simple, ordinary, linear, quadratic, and polynomial, etc. [17]. The function $Z(\mathbf{x})$ is the realisation of the Gaussian process with zero mean and nonzero covariance; $Z(\mathbf{x})$ is expressed as

$$cov\left(Z(\mathbf{x}_i), Z(\mathbf{x}_j)\right) = \sigma^2 R\left(\mathbf{x}_i - \mathbf{x}_j \middle| \boldsymbol{\theta}\right), \tag{2}$$

where σ^2 is the process variance and $R\left(\mathbf{x}_\mathrm{i} - \mathbf{x}_\mathrm{j} \middle| \boldsymbol{\theta}\right)$ is the spatial correlation function with known or unknown correlation parameters $\boldsymbol{\theta}$. The Gaussian process assumes that the correlation between $Z(\mathbf{x}_i)$ and $Z\left(\mathbf{x}_j\right)$ is a function of the distance between $\mathbf{x}_i$ and $\mathbf{x}_j$. Several correlation functions can be used in the Kriging model, e.g., linear, exponential, squared exponential, and Matérn, etc. [17].

It should be noticed from Equation (1) that the first term $\boldsymbol{\beta}^T \mathbf{f}(\mathbf{x})$ provides a global model which is represented by various basic functions, and the second term $Z(\mathbf{x})$ creates a localized deviation between the global model and the exact model. Therefore, the Kriging model can successfully interpolate the n data points and this method is flexible due to various basic and correlation functions.

The output $Y(\mathbf{x}_0)$, where $\mathbf{x}_0$ is a new input point, can be predicted based on the input points $\mathbf{X} = (\mathbf{x}_1, \mathbf{x}_2, \ldots, \mathbf{x}_n)$ and the corresponding computer output $\mathbf{Y}^n = (Y(\mathbf{x}_1), Y(\mathbf{x}_2), \ldots, Y(\mathbf{x}_\mathrm{n}))^T$, given as

$$\begin{pmatrix} Y(\mathbf{x}_0) \\ \mathbf{Y}^n \end{pmatrix} \sim N_{n+1}\left(\begin{pmatrix} \mathbf{f}_0^T \\ \mathbf{F} \end{pmatrix}\boldsymbol{\beta}, \sigma^2 \begin{pmatrix} 1 & r_0^T \\ r_0 & \mathbf{R} \end{pmatrix}\right), \tag{3}$$

where $\mathbf{f}_0 = f(\mathbf{x}_0)$ and $\mathbf{F} = f_j(\mathbf{x}_i)$ are the regression function vector of the predicted data and the regression function matrix of the training data, respectively, r_0 is the correlation function vector of among $\mathbf{Y}^n$ and $Y(\mathbf{x}_0)$, $\mathbf{R}$ is the correlation matrix of among $\mathbf{Y}^n$. Then, the conditional mean and the conditional variance of the Gaussian process of $Y(\mathbf{x}_0)$ are extracted from Equation (3), i.e.,

$$\mu_{Y(\mathbf{x}_0)} = \left(\mathbf{f}_0^T \hat{\boldsymbol{\beta}} + r_0^T R^{-1}(\mathbf{Y}^n - F\hat{\boldsymbol{\beta}})\right) \text{ and} \tag{4}$$

$$\sigma^2{}_{Y(\mathbf{x}_0)} = \sigma^2(1 - \boldsymbol{r}_0^T\boldsymbol{R}^{-1}\boldsymbol{r}_0 + (\boldsymbol{F}^T\boldsymbol{R}^{-1}\boldsymbol{r}_0 - \boldsymbol{f}_0)^T(\boldsymbol{F}^T\boldsymbol{R}^{-1}\boldsymbol{F})^{-1}(\boldsymbol{F}^T\boldsymbol{R}^{-1}\boldsymbol{r}_0 - \boldsymbol{f}_0)), \tag{5}$$

$$\text{with } \hat{\boldsymbol{\beta}} = (\mathbf{F}^T\mathbf{R}^{-1}\mathbf{F})^{-1}\mathbf{F}^T\mathbf{R}^{-1}\mathbf{Y}^n. \tag{6}$$

Because the hyperparameter vector θ is unknown, an estimation method needs to be used to obtain a Kriging model and the estimation. The estimation is obtained by solving an optimization problem. In this paper, the maximum likelihood estimation is adopted to identify the vectors $\boldsymbol{\beta}$, σ^2, and θ, given as

$$L(\boldsymbol{\beta}, \sigma^2, \theta|\mathbf{Y}^n) = \frac{(\det\mathbf{R})^{\frac{1}{2}}}{(2\pi\sigma^2)^{\frac{n}{2}}} \exp\left(-\frac{1}{2\sigma^2}(\mathbf{Y}_\mathrm{n} - \mathbf{F}\boldsymbol{\beta})^{\mathrm{T}}\mathbf{R}^{-1}(\mathbf{Y}_\mathrm{n} - \mathbf{F}\boldsymbol{\beta})\right). \tag{7}$$

By maximizing the quantity in Equation (3), the analytical estimates of $\boldsymbol{\beta}$ and σ^2 that are functions of θ can be are obtained [16,17].

2.2. Metamodel Validation

The predictive performance of the Kriging model can be evaluated by the error between observed and predicted responses. The leave-one-out (LOO) cross-validation method is the most commonly used, in which one point is randomly selected for the validating purpose while the other points are used for training the metamodel. This procedure is repeated until all the points are used as a test dataset. Therefore, to perform the LOO cross-validation, one point $\mathbf{x}_k$ from the DOE is removed and the metamodel $\hat{\mathbf{Y}}_{(-k)}(\mathbf{x}_k)$ is subsequently built from the remaining points of the DOE. The root mean square error (RMSE) quantifying the difference between the predictive and observed responses from the cross-validation and the coefficient of determination R^2 are calculated as

$$\mathrm{RMSE} = \sqrt{\frac{\sum_{k=1}^{n}\left[Y(\mathbf{x}_k) - \hat{\mathbf{Y}}_{(-k)}(\mathbf{x}_k)\right]^2}{n}} \text{ and} \tag{8}$$

$$\mathrm{R}^2 = 1 - \frac{1}{n}\frac{\sum_{k=1}^{n}\left[Y(\mathbf{x}_k) - \hat{\mathbf{Y}}_{(-k)}(\mathbf{x}_k)\right]^2}{\mathrm{Var}\ (\mathbf{Y}^\mathrm{n})}, \tag{9}$$

where $\mathrm{Var}(\mathbf{Y}^\mathrm{n})$ is the estimated variance of the actual responses. In addition, the relative maximum absolute error (RMAE) can be also determined, which measures the extent of the local fitting error, given as

$$\mathrm{RMAE} = \frac{\max\left|Y(\mathbf{x}_k) - \hat{\mathbf{Y}}_{(-k)}(\mathbf{x}_k)\right|}{\mathrm{Std}(\mathbf{Y}^\mathrm{n})}, \tag{10}$$

where $\mathrm{Std}(\mathbf{Y}^\mathrm{n})$ is the standard deviation of the actual responses.

2.3. Fragility Analysis Procedure

The entire procedure for evaluating fragility functions of RC bridges based on Kriging metamodel is described in Figure 1. The steps are summarized as the following:

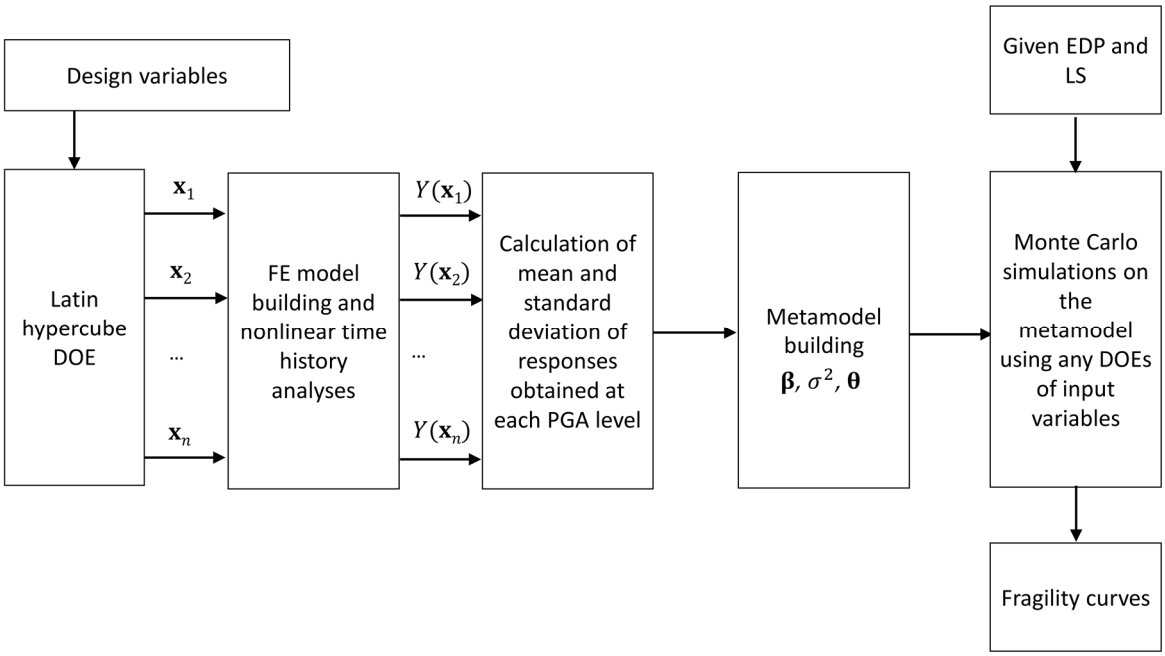

Figure 1. Kriging metamodel-based fragility evaluation procedure.

1. Design variables are first defined. In the case of RC bridges, uncertainties of material and geometry parameters are commonly defined by a range of design values. The ground motion uncertainty is also considered by a range of peak ground acceleration (PGA). To reduce the computational cost, a screening study is often conducted to define which modeling parameters are significant [18]. However, this step is ignored in this study; the sensitivity of some modeling parameters will be assessed after the metamodeling has been built.
2. The next step of the framework is the generation of samples of input random variables using a proper DOE technique. Among different sampling methods, Latin hypercube sampling (LHS) is often suggested for Kriging metamodeling [19] and is selected in this study.
3. In the subsequent step, nonlinear time history dynamic analyses are performed on the FE model of generated bridges subjected to different levels of ground motions. Peak responses are then measured for each simulation. Because each ground motion is scaled with respect to the PGA values in the DOE, hence the total of observed responses from the time history analyses is (n_{sample} x $n_{ground\ motion}$). To be a suitable input for the metamodel, a deterministic observed response for each sample is need; therefore, statistics in terms of the mean and standard deviation (Std) of the responses are calculated for each sample of the DOE, where the Std represents the variation of the response due to the frequency content. With emphasizing on the damage of the column bent, in this study, the column drift ratio will be recorded from the analyses.
4. Two Kriging metamodels are built for the mean and Std of the observed responses, and then a composed Kriging metamodel is then developed assuming a lognormal distribution [14,15].
5. Seismic fragility curves are finally derived by Monte Carlo simulations, given an engineering demand parameter (EDP) and its limit state (LS) that are conducted based on a close-formed Kriging metamodel. The flexibility of the Kriging model allows deriving fragility curves with any DOEs of any input conditions of the random variables.

3. Seismic Fragility Analysis of Case Study

3.1. Description of Case Study, Input Variables and Numerical Modeling

A class of single-bent RC highway bridges with a box girder is selected as a case study, as shown in Figure 2. This is a typical overpass bridge in California and has been evaluated by numerous studies, e.g., [20–23]. Analyses are performed on the DOE of six modeling parameters involving bridge material and geometry properties, detailed in Table 1 along with ranges assigned to each of the parameters. In the later DOE, all the parameters are assumed to follow the uniform distribution. The superstructure is a multiple-cell box girder, its width B and depth D_s are deterministic (i.e., 11.9 and 1.83 m, respectively). The span length L, the column height H, and the column diameter D_c are varied. Furthermore, material properties for both the concrete and reinforcing steel, including the reinforcement nominal yield strength f_y, the concrete nominal strength f'_c, and the longitudinal reinforcement ratio ρ_l, are also varied, making in total 60 experimental designs of the input random variables. It should be noticed that the ranges of the parameters listed in Table 1 are chosen according to Mackie and Stojadinovic [20] and Huang et al. [21].

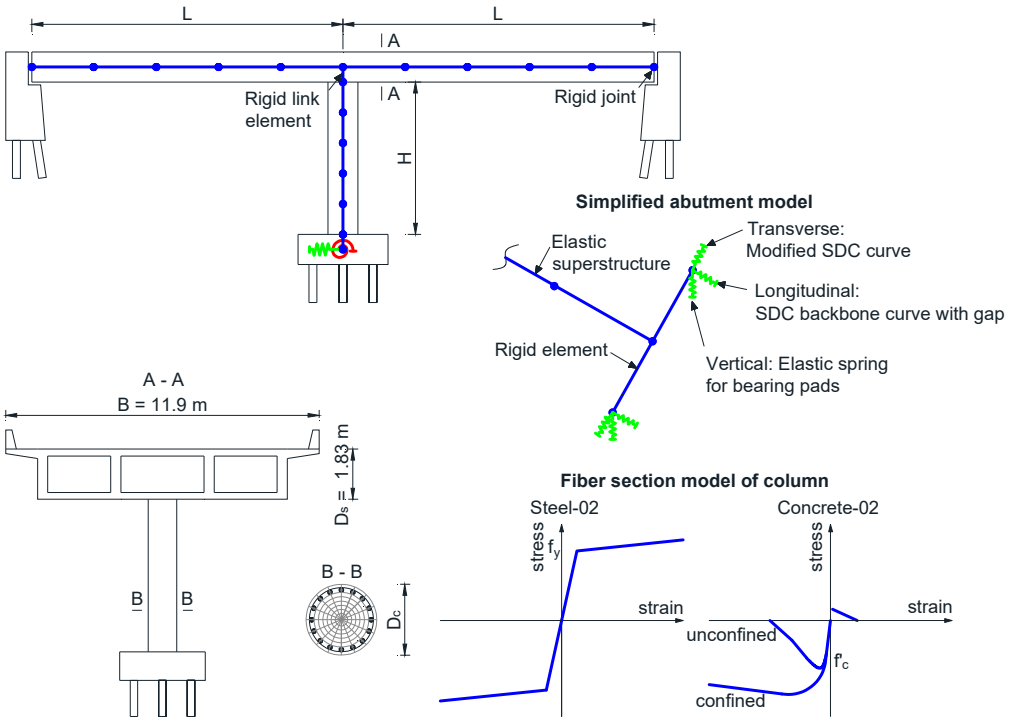

Figure 2. Two-span, single-bent RC bridge model.

Table 1. Ranges of the design parameters for single-bent RC highway bridges.

Input Variable	Range
Span length (L)	18–55 m
Deck width (B)	11.9 m
Deck depth (D_s)	1.83 m
Colum height (H)	5–11 m
Column diameter (D_c)	1–2 m
Longitudinal reinforcement ratio (ρ_l)	1–4%
Steel strength (f_y)	470–655 MPa
Concrete strength (f'_c)	20–55 MPa
Steel weight	76,973 N/m^3
Concrete weight	23,563 N/m^3

The base bridge is modeled using the FE OpenSees software [24]. The discrete FE model is also shown in Figure 2. The detail of the modeling approach is as follows:

1. **Deck:** The deck is modeled using elastic beam-column elements discretized into five separate elements along each clear span. Elastic material properties are assigned to all the elements with the assumption is that the deck behavior under the seismic event falls in the elastic range. The material and section properties used to modeled the RC deck with the elastic behavior are is shown in Table 2; in this study, these parameters are set as deterministic.

Table 2. Deck properties.

Deck Property	Value
Young modulus	28,000 MPa
Shear modulus	11,500 MPa
Unit weight	23.571 kN/m^3
Area cross-section	6.328 m^2
Moment of inertia about the horizontal axis	3.073 m^4
Moment of inertia about the horizontal axis	71.823 m^4
Torsion constant	8.444
Weight per unit length	149.152 kN/m

2. **Pier:** The circular column pier is modeled as nonlinear beam-column elements with the fiber section, where the Concrete-02 and Steel-02 uniaxial materials are used to model the nonlinear behavior of the concrete and steel of the column (see fiber section model in Figure 2). Concrete-02 is a uniaxial material with linear tension softening, while Steel-02 is a uniaxial Giuffré-Menegotto-Pinto material that allows for isotropic strain hardening. The material parameters of Concrete-02 are obtained from the Mander constitutive relationships [25] for confined and unconfined concretes. In detail, for cover concrete, the concrete unconfined strength is equal to f'_c, the concrete strain at maximum strength equals 0.002, the concrete crushing strength is zero, and the concrete strain at crushing strength equals 0.006. For core concrete of circular column cross-sections, the modeling parameters are defined according to the Mander model. As boundary conditions, the column ends are connected to the superstructure and the footing by rigid link elements. The footing is supported by translational and rotational springs as recommended by Nielson and DesRoches [26] that can be considered the stiffness of an individual pile and the stiffness of the pile group. In this study, the springs are modelled to be very stiff, neglecting the soil-structure interaction (SSI) effect. Influencing the SSI into the numerical model considering the interaction between the pile group and soil will enhance considerably the model accuracy [22,23]; however, this is out of scope within the study since the focusing is on the fragility analysis framework.
3. **Abutment:** A simplified abutment model is used with the general scheme presented in Figure 2. This abutment model consists of a rigid element connected through a rigid joint to the superstructure, with defined longitudinal, transverse, and vertical behaviors at each end. The calculation of these spring behaviors for the abutment model has followed the work by Mackie et al. [20,27].

The Rayleigh damping is employed in the model, which takes form as

$$\mathbf{C} = a_m \mathbf{M} + a_k \mathbf{K}, \tag{11}$$

where **M** is the mass matrix, **C** is the damping matrix, and **K** is the initial stiffness matrix. Damping coefficients a_m and a_k can be determined from the relationship

$$\xi = \frac{a_m}{4\pi f} + a_k \pi f, \tag{12}$$

where ξ is the damping ratio and f is the frequency. From Equation (12), damping coefficients are defined by specifying two frequencies and damping ratio values. In this study, the first two-frequency range with 1 and 6 Hz, and 2% damping ratio are assumed.

The LHS method is used to generate samples of the random variables in Table 1. This method has been demonstrated as the most suitable with the Kriging model in constructing surrogate models [19]. A total of 60 bridge samples is generated; this number of samples is chosen according to the work of Huang et al. [21]. The modal analysis is first performed for the sample set. Longitudinal behavior is described by the first two natural periods, i.e., T_1 = 0.181-0.830 s and T_2 = 0.167-0.603 s. In later nonlinear structural dynamic analyses, the governing equations of the system are discretized by Newmark time integration and then is solved via the KrylovNewton algorithm [24].

3.2. Ground Motion Selection

The selection of a suite of ground motions to be used as input for nonlinear dynamic analysis is also a challenge within the PBEE framework. The number of suitable ground motions depends on which fragility analysis method to be adopted. Usually, a large number of records is used for the structural dynamic analysis to build an appropriate probabilistic seismic demand model, and in the context of a surrogate model, there is no specific standard for the ground motion selection.

In this paper, unscaled ground motion records are selected, which have been demonstrated as a suitable input for analytical fragility assessments [28]. For a Kriging-based metamodel, a limited number of records can be used [4], hence in this study, a set of 20 records is selected from the PEER ground motion database [29]. The characteristics of the records are summarized in Table 3; these records are mainshock free-field recordings. The soil of the record stations is characterized by stiff soil conditions, which has average shear wave velocities of the top 30 m of soil ($V_{s,30}$) from 360 to 760 m/s. The set of records covers a wide range of the moment magnitudes (M_W) between 5.1 and 6.9. The Joyner-Boore distances (R_{jb}) are limited under 20 km for near-source records. The response spectra of all selected records along with their mean spectrum and the range of the bridge fundamental periods are shown in Figure 3.

Table 3. Selected PEER ground motion records.

ID	Earthquake Name	Year	Station	M_W	R_{jb} (km)	$V_{s,30}$ (m/sec)
1	Irpinia Italy-01	1980	Bagnoli Irpinio	6.9	8.14	649.67
2	Irpinia Italy-01	1980	Sturno	6.9	6.78	382
3	Irpinia Italy-02	1980	Calitri	6.2	8.81	455.93
4	Corinth Greece	1981	Corinth	6.6	10.27	361.4
5	Northridge-01	1994	Sunland—Mt Gleason A	6.69	12.38	402.16
6	Chi-Chi Taiwan-03	1999	TCU084	6.2	3.68	665.2
7	Tottori Japan	2000	SMNH01	6.61	5.83	446.34
8	Parkfield-02 CA	2004	Parkfield—Upsar 03	6	9.49	440.59
9	Parkfield-02 CA	2004	Parkfield—Upsar 05	6	9.14	440.59
10	Parkfield-02 CA	2004	Parkfield—Upsar 06	6	9.14	440.59
11	Parkfield-02 CA	2004	Parkfield—Upsar 08	6	8.93	440.59
12	Parkfield-02 CA	2004	Parkfield—Upsar 09	6	8.86	466.12
13	Parkfield-02 CA	2004	Parkfield—Upsar 12	6	9	466.12
14	Parkfield-02 CA	2004	Parkfield—Upsar 13	6	9	466.12
15	Chuetsu-oki Japan	2007	Joetsu K. Kakizaki	6.8	9.43	383.43
16	Chuetsu-oki Japan	2007	Tani Kozima Nagaoka	6.8	5	561.59
17	Iwate Japan	2008	IWTH24	6.9	3.1	486.41
18	Iwate Japan	2008	MYG005	6.9	10.71	361.24
19	Iwate Japan	2008	Mizusawaku Interior	6.9	7.82	413.04
20	Iwate Japan	2008	Kurihara City	6.9	12.83	512.26

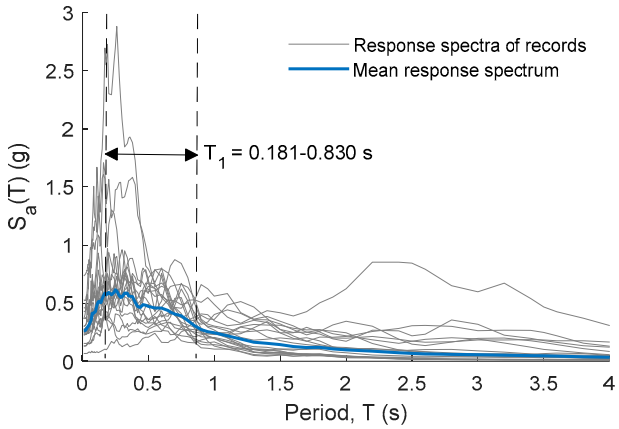

Figure 3. Response spectra of the selected records.

3.3. Construction of the Kriging Metamodel Using Nonlinear Time History Analyses

As a result of the LHS, 60 samples with different combinations of the modeling parameter and *PGA* are generated. Each sample is modeled using the three-dimensional FE model presented in Section 3.1 and subjected to 20 selected records in Section 3.2. The records are respectively scaled to *PGA* values in the DOE. Therefore, 1200 simulations are carried out. An example of the time history data in terms of the drift ratio of the column top and its drift ratio-shear force hysteretic behavior is shown in Figure 4. The response quantities are measured from the analysis of Sample 1 and Sample 60 subjected to Record 1; where Sample 1 is comprised by H = 6.730 m, L = 34.315 m; D_c = 1.150 m, f_c' = 299.310 MPa; f_y = 475.369 MPa; ρ_l = 3.009; PGA = 0.540 and Sample 60 is comprised by H = 7.563 m, L = 45.776 m; D_c = 1.035 m, f_c' = 205.263 MPa, f_y = 545.532 MPa; ρ_l = 2.186; PGA = 0.693. It can be seen that Sample 60 is more vulnerable to seismic action because of the weak column and high seismic intensity. The peak drift ratio measured for Sample 60 is about 2.7% while that of Sample 1 is about 0.8%.

Similarly, the peak seismic responses in terms of the drift ratio are measured for all the samples, as shown in Figure 5. The analyses consider the variation of the frequency content by scaling each ground motion record to different *PGA* values from the DOE. At each *PGA* value, the responses vary due to the effect of the frequency content from different ground motions. Therefore, the transient analysis results are not able to use as training data for the Kriging model; thus, the mean and Std values of the responses at each *PGA* level are used instead.

Kriging metamodels are built for the mean and Std responses using the Matlab-based UQLAB software framework [17]. To select the best suitable trend (or basic function) for the model, a parametric study on the effectiveness of different trends is first conducted, where the correlation function is set as the default. The leave-one-out (LOO) cross-validation method is used to evaluate the error of the model. The results in terms of RMSE, R^2, and RMAE are shown in Table 4. It can be seen from the table that all the trends show their ability in predicting the mean of the structural response with low error and high determination coefficient ($R^2 > 0.96$). A careful reader can see that the 2nd-degree polynomial function shows its best performance. Hence in the following evaluation, the 2nd-degree polynomial function is chosen. The correlation type and the correlation family are given by the Separable correlation function and the Matern 3/2 kernel function, respectively. The maximum likelihood estimation in Equation (7) is adopted to estimate the hyperparameters. Once the two Kriging models for both mean and Std of the responses are built, the composed Kriging model is then obtained that is assumed to follow a lognormal distribution [4].

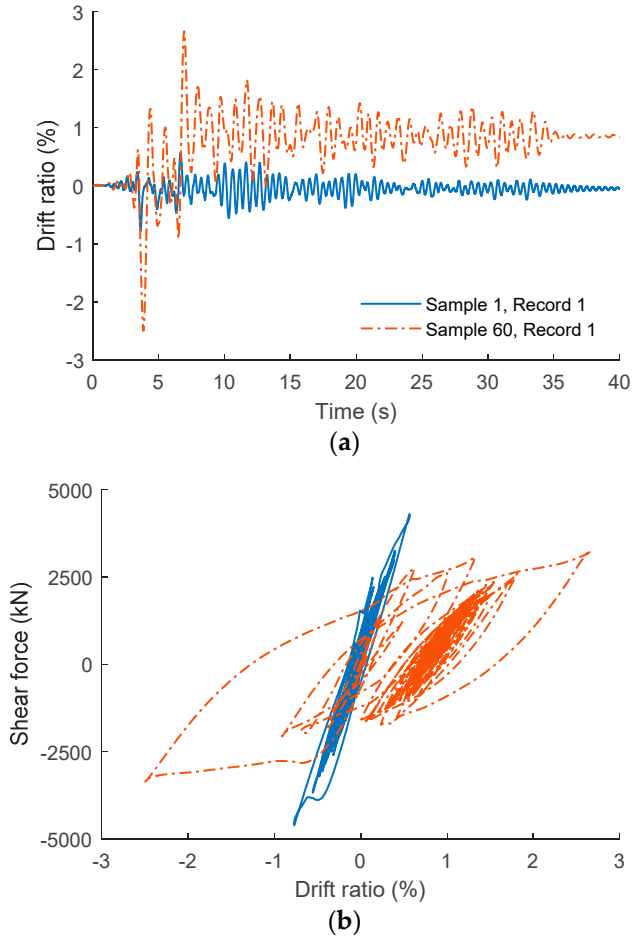

Figure 4. Example of nonlinear time history analysis results: (**a**) Time history data of column top drift ratio and (**b**) Hysteretic behavior in terms of column top drift ratio and base shear.

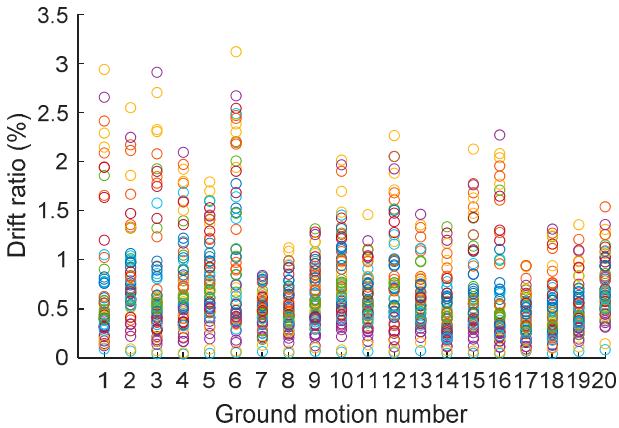

Figure 5. Maximum column drifts collected as observed training data.

3.4. Fragility Analysis

With a particular focus on the performance of the column, its EDP is quantified in terms of the maximum drift ratio. The damage states according to the drift ratio EDP are damage with initial cracking (DS1), cover concrete spalling (DS2) and column failure (DS3). For this typical reinforced concrete column with a circular cross-section, three damage states and their median drift ratios for the LS are defined [20], as shown in Table 5.

Table 4. Basic function comparison by the LOO error estimation.

Basic Function	RMSE	R^2	RMAE
Ordinary	0.124	0.965	0.778
Linear	0.117	0.969	0.649
Quadratic	0.090	0.981	0.981
1st-degree polynomial	0.119	0.968	0.679
2nd-degree polynomial	0.087	0.983	0.357

Table 5. Damage states and corresponding limit states for the column drift EDP.

Damage State	Damage State Limit Description	Median Drift Ratio for the Limit State (%)
DS1	Negligible damage with initial cracking	0.23
DS2	Cover concrete spalling	1.64
DS3	Column failure	6.72

Given the limit states, the fragility curves of the corresponding failure modes are derived based on Monte Carlo simulations which are performed on the composed Kriging metamodel. Given a range of PGA values varying from 0.01 g to 1.5 g with a step size of 0.01, the simulated are repeated for each PGA in the range which incorporates the modeling parameters to generate a new DOE. The post-processing of the data on a large number of samples, i.e., 10,000 samples for each PGA, results in fragility curves of the three failure modes of the column, as shown in Figure 6. To ensure a smooth curve and a reliable result, a large number of samples must be used; this is only possible in the context of an available metamodel. The fragility curves presented in Figure 6 show the probabilities of exceeding the drift limits of the column. For DS1, the 50% probability of failure corresponds to a PGA value of around 0.15 g, while this figure for DS2 is about 1.3 g. The probability of occurrence of DS3 is very limited.

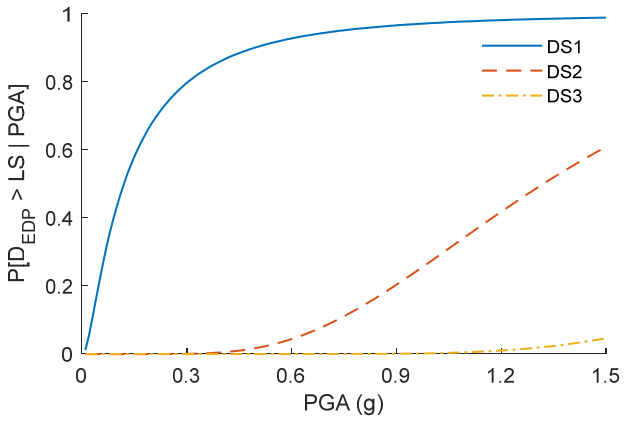

Figure 6. Fragility curves for different damage states of the column considering the range of the input random variables in Table 1.

In addition, the advance of the metamodel is its flexibility to rapidly draw fragility curves for different input conditions. For examples, it can easily assess the effect of one input variable on the seismic fragility of the column without re-construction and re-evaluation of the model. For example, by considering the lower and upper values of one of the geometry variables, i.e., the column height, the span length, or the column diameter, corresponding fragility curves for the DS1 and DS2 are respectively obtained as shown in Figures 7–9. It is noticed that the remaining variables are kept in the range illustrated in Table 1.

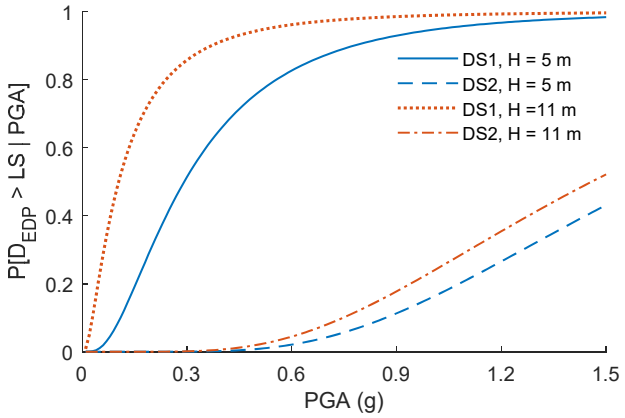

Figure 7. Fragility curves for DS1 and DS2 of the column with the lower and upper values of the column height.

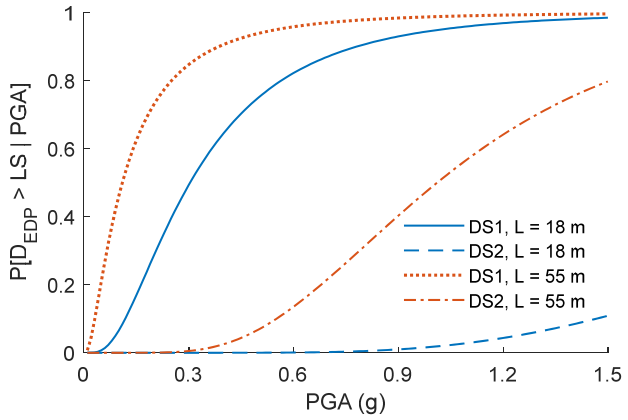

Figure 8. Fragility curves for DS1 and DS2 of the column with the lower and upper values of the span length.

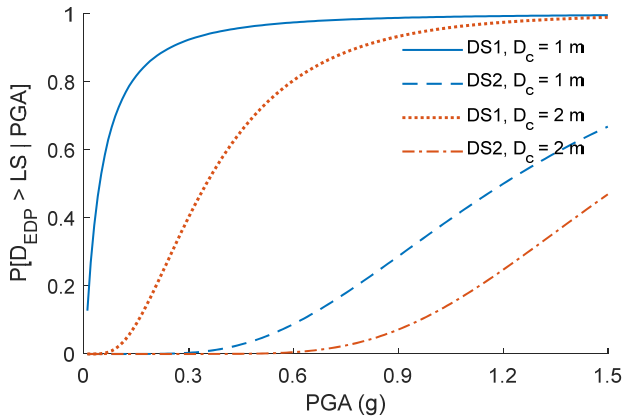

Figure 9. Fragility curves for DS1 and DS2 of the column with the lower and upper values of the column diameter.

The findings from the analysis show that the geometry parameters are much sensitive to the fragility curves of the two damage states. In Figure 7, the 50% probability of the column damage with initial cracking (i.e., DS1) corresponding for D_c = 1 and 2 m are 0.1 g and 0.3 g, respectively. This observation is similar to the case in which two different span lengths (i.e., 18 and 55 m) are considered (see Figure 8), whereas the increase of the column diameter from 1 m to 2 m significantly reduces the probability of the column failure, as shown in Figure 9. Also of note is that there is a remarkable change in the fragility curve of

the cover concrete spalling (i.e., DS2) for the lower and upper span lengths. This difference is considerable in the cases of the column diameter, especially for the column height cases, the fragility curves of the lower and upper bound are quite close. The sensitivity analysis can be further expanded to the material parameters by setting one of the parameters as deterministic and performing similarly the analysis based on the developed metamodel.

4. Conclusions

This paper presented a computationally efficient framework for the seismic fragility evaluation of a class of RC highway bridges. The framework used a probabilistic metamodel that is built based on the Kriging approach. By application to a case study of typical single-bent RC highway bridges, this framework offered a limited of simulations to obtain seismic fragility curves of the bridge class and showed its capacity in rapidly predicting fragility curves for different input conditions of the random variables without re-construction and re-evaluation of the numerical model simulation.

The metamodel was developed based on the LHS DOE of seven input random variables and the output responses obtained from time history analyses of the resulting 60 FE models subjected to 20 near-source natural records; this led to a total of 1200 simulations. Fragility curves of three damage states of the column were obtained using Monte Carlo simulations carried out on the closed-form of the Kriging metamodel. Results of the analysis showed the good seismic performance of the column bent of this highway bridge class that was recognized a low probability of failure.

In addition, using a cross-validation method, a comparative study on the selection of the trend function in the performance of the metamodel was performed. The 2nd-degree polynomial function showed the best performance among others by comparing three predictive error indicators, i.e., RMSE, R^2, and RMAE.

The capability of the present procedure of obtaining fragility curves for different input conditions was also demonstrated. By setting one of the input variables as deterministic with its lower and upper bound, fragility curves of different damage stages could be rapidly built without re-construction and re-evaluation of the numerical model. Therefore, the fragility sensitivity of some geometry modeling parameters was assessed. The findings from the analysis showed significant effects of the geometry parameters, such as the column height, the span length, and the column diameter, on the seismic fragility curves of the column.

The fragility curves were generated for the specific bridge class, i.e., single-bent RC highway bridges with a circular column; however, the finding framework can further apply to any type of bridges considering different sources of uncertainty.

Author Contributions: Conceptualization, P.H.H., H.N.P. and F.P.; methodology, P.H.H., H.N.P. and F.P.; software, H.N.P. and D.T.N.; formal analysis, H.N.P. and D.T.N.; investigation, H.N.P. and D.T.N.; writing—original draft preparation, P.H.H., H.N.P. and D.T.N.; writing—review and editing, H.N.P. and F.P. All authors have read and agreed to the published version of the manuscript.

Funding: This work was supported by The University of Danang, University of Science and Technology, code number of Project: T2021-02-15.

Institutional Review Board Statement: Not applicable.

Informed Consent Statement: Not applicable.

Data Availability Statement: The data used to support the findings of this study are available from the corresponding author upon request.

Conflicts of Interest: The authors declare no conflict of interest.

References

1. Muntasir Billah, A.H.M.; Shahria Alam, M. Seismic fragility assessment of highway bridges: A state-of-the-art review. *Struct. Infrastruct. Eng.* **2015**, *11*, 804–832. [CrossRef]
2. Segura, R.; Padgett, J.E.; Paultre, P. Metamodel-Based Seismic Fragility Analysis of Concrete Gravity Dams. *J. Struct. Eng.* **2020**, *146*, 04020121. [CrossRef]
3. Du, A.; Padgett, J.E. Investigation of multivariate seismic surrogate demand modeling for multi-response structural systems. *Eng. Struct.* **2020**, *207*, 110210. [CrossRef]
4. Phan, H.N.; Paolacci, F.; Di Filippo, R.; Bursi, O.S. Seismic vulnerability of above-ground storage tanks with unanchored support conditions for Na-tech risks based on Gaussian process regression. *Bull. Earthq. Eng.* **2020**, *18*, 6883–6906. [CrossRef]
5. Xie, Y.; Ebad Sichani, M.; Padgett, J.E.; DesRoches, R. The promise of implementing machine learning in earthquake engineering: A state-of-the-art review. *Earthq. Spectra* **2020**, *36*, 1769–1801. [CrossRef]
6. Forrester, A.I.J.; Sóbester, A.; Keane, A.J. *Engineering Design Via Surrogate Modelling: A Practical Guide*; Wiley: Chichester, West Sussex, UK, 2008.
7. Asher, M.J.; Croke, B.F.W.; Jakeman, A.J.; Peeters, L.J.M. A review of surrogate models and their application to groundwater modelling. *Water Resour. Res.* **2015**, *51*, 5957–5973. [CrossRef]
8. Hu, J.; Shen, E.; Gu, Y. Simulating Performance Risk for Lighting Retrofit Decisions. *Buildings* **2015**, *5*, 650–667. [CrossRef]
9. Le, T.T. Surrogate Neural Network Model for Prediction of Load-Bearing Capacity of CFSS Members Considering Loading Eccentricity. *Appl. Sci.* **2020**, *10*, 3452. [CrossRef]
10. Choi, W.; Radhakrishnan, K.; Kim, N.-H.; Park, J.S. Multi-Fidelity Surrogate Models for Predicting Averaged Heat Transfer Coefficients on Endwall of Turbine Blades. *Energies* **2021**, *14*, 482. [CrossRef]
11. Rasmussen, C.E.; Williams, C.K.I. *Gaussian Processes for Machine Learning*; The MIT Press: Cambridge, MA, USA, 2006.
12. Kameshwar, S.; Padgett, J.E. Multi-hazard risk assessment of highway bridges subjected to earthquake and hurricane hazards. *Eng. Struct.* **2014**, *78*, 154–166. [CrossRef]
13. Ghosh, J.; Padgett, J.E.; Dueñas Osorio, L. Surrogate modeling and failure surface visualization for efficient seismic vulnerability assessment of highway bridges. *Probab. Eng. Mech.* **2013**, *34*, 189–199. [CrossRef]
14. Zhang, Y.; Wu, G. Seismic vulnerability analysis of RC bridges based on Kriging model. *J. Earthq. Eng.* **2017**, *23*, 242–260. [CrossRef]
15. Gidaris, I.; Padgett, J.E.; Misra, S. Probabilistic fragility and resilience assessment and sensitivity analysis of bridges incorporating aftershock effects. *Sustain. Resilient Infrastruct.* **2020**, *5*, 1–23. [CrossRef]
16. Santner, T.J.; Williams, B.; Notz, W. *The Design and Analysis of Computer Experiments*; Springer series in Statistics; Springer: Berlin/Heidelberg, Germany, 2003.
17. Lataniotis, C.; Marelli, S.; Sudret, B. *UQLab User Manual—Kriging (Gaussian Process Modelling)*; Report UQLab-V11-105; Risk, Safety & Uncertainty Quantification, ETH Zurich: Zurich, Switzerland, 2018.
18. Phan, H.N.; Paolacci, F.; Alessandri, S. Enhanced Seismic Fragility Analysis of Unanchored Steel Storage Tanks Accounting for Uncertain Modeling Parameters. *ASME J. Press. Vessel Technol.* **2019**, *141*, 010903. [CrossRef]
19. Kleijnen, J.P.C. Regression and Kriging metamodels with their experimental designs in simulation: A review. *Eur. J. Oper. Res.* **2017**, *256*, 1–16. [CrossRef]
20. Mackie, K.R.; Stojadinovic, B. *Fragility Basis for California Highway Overpass Bridge Seismic Decision Making*; Report no. 2005/02; Pacific Earthquake Engineering Research Center: Berkeley, CA, USA, 2005.
21. Huang, Q.; Gardoni, P.; Hurlebaus, S. Probabilistic Seismic Demand Models and Fragility Estimates for Reinforced Concrete Highway Bridges with One Single-Column Bent. *J. Eng. Mech.* **2010**, *136*, 1340–1353. [CrossRef]
22. Mackie, K.R.; Lu, J.; Elgamal, A. Performance-based earthquake assessment of bridge systems including ground-foundation interaction. *Soil Dyn. Earthq. Eng.* **2012**, *42*, 184–196. [CrossRef]
23. Forcellini, D. Cost assessment of isolation technique applied to a benchmark bridge with soil structure interaction. *Bull. Earthq. Eng.* **2017**, *15*, 51–69. [CrossRef]
24. McKenna, F.; Fenves, G.L.; Scott, M.H. *Open System for Earthquake Engineering Simulation*; University of California: Berkeley, CA, USA, 2000.
25. Mander, J.B.; Priestley, M.J.N.; Park, R. Theoretical stress-strain model for confined concrete. *J. Struct. Eng.* **1998**, *114*, 1804–1826. [CrossRef]
26. Nielson, B.G.; DesRoches, R. Influence of modeling assumptions on the seismic response of multi-span simply supported steel girder bridges in moderate seismic zones. *Eng. Struct.* **2006**, *28*, 1083–1092. [CrossRef]
27. Aviram, A.; Mackie, K.R.; Stojadinovic, B. Effect of abutment modeling on the seismic response of bridge structures. *Earthq. Eng. Eng. Vib.* **2008**, *7*, 395–402. [CrossRef]
28. Jalayer, F.; Ebrahimian, H.; Miano, A.; Manfredi, G.; Sezen, H. Analytical fragility assessment using unscaled ground motion records. *Earthq. Eng. Struct. Dyn.* **2017**, *46*, 2639–2663. [CrossRef]
29. Phan, H.N.; Paolacci, F.; Bursi, O.S.; Tondini, N. Seismic fragility analysis of elevated steel storage tanks supported by reinforced concrete columns. *J. Loss Prev. Process Ind.* **2017**, *47*, 57–65. [CrossRef]